Nondestructive Evaluation of the Characteristics of Degraded Materials Using Backward Radiated Ultrasound

Sung D. Kwon

*Department of Physics, Andong National University, 388 Songchundong, Andong,
Kyungbuk 760-749, Korea*

Sung J. Song, Dong H. Bae*, Young Z. Lee

*School of Mechanical Engineering, Sungkyunkwan University, 300 Chunchundong, Suwon,
Kyunggi-do 440-746, Korea*

The frequency dependency of Rayleigh surface wave is investigated indirectly by measuring the angular dependency of the backward radiation of the incident ultrasonic wave in two kinds of degraded specimens by scuffing or corrosion. Then, the frequency dependency is compared with the residual stress distribution or the corrosion-fatigue characteristics for the scuffed or corroded specimens, respectively. The width of the backward radiation profile increases with the increase of the variation in residual stress distribution for the scuffed specimens. In the corroded specimens, the profile width decreases with the increase of the effective aging layer thickness and is inversely proportional to the exponent, m, in the Paris' law that can predict the crack size increase due to fatigue. The result observed in this study demonstrates high potential of backward radiated ultrasound as a tool for nondestructive evaluation of subsurface gradient of material degradation generated by scuffing or corrosion.

Key Words : Backward Radiated Ultrasound, Residual Stress Distribution, Corrosion Fatigue Characteristic, Scuffing, Crack Growth rate, Nondestructive Evaluation

1. Introduction

Characterization of subsurface gradients of degraded materials is one of the fundamental issues for the reliability evaluation of various mechanical components. This is especially crucial for components exposed to scuffing or corrosion.

Rayleigh surface waves that can penetrate to some depth below the surface with an exponential profile (Viktorov, 1967) can be used for the investigation of such gradients in degraded materials. When a specimen with uniform acoustical properties undergoes surface treatments

* Corresponding Author,
  E-mail : bae@yurim.skku.ac.kr
  TEL : +82-31-290-7443; **FAX :** +82-31-295-1937
  School of Mechanical Engineering, Sungkyunkwan University 300 Chunchun-dong, Jangan-ku, Suwon, Kyunggi-do 440-746, Korea. (Manuscript **Received** December 17, 2001; **Revised** June 10, 2002)

such as heating, implantation and coating, the substrate develops variations of density and elastic modulus with depth, i.e., subsurface gradients. In such a case, the substrate is said to be mechanically perturbed and the subsurface gradient causes wave dispersion (Szabo, 1975; Kwon and Kim, 1987).

When an incident broadband pulse at an arbitrary angle of incidence reflects, a Rayleigh wave is generated, if the phase of the incident beam matches that of the surface wave. In this circumstance, the leaky wave will interfere destructively with the reflected beam producing non-specular reflection field (Bertoni and Tamir, 1973). When the pulse-echo method is used at an arbitrary angle on the liquid/solid boundary, the received signal is called the ultrasonic backscattering. Angular dependence of the ultrasonic backscattering involves the coherent backward radiation returning along the incident direction from

backward propagating surface waves. Previous study (Kim et al., 1999) showed that backward radiation could be used to assess the micro-structures in the surface region. Partial dispersion relations of layered substrates were evaluated from the angular dependence of backward radiation (Kwon et al., 2000).

In this paper, the frequency dependency of Rayleigh surface wave is investigated indirectly by measuring the angular dependency of backward radiation of the incident ultrasonic wave in two kinds of degraded specimens : 1) aged specimens, and 2) worn specimens. And then, the results with the two specimens are compared with the corrosion-fatigue characteristics and residual stress distributions, respectively.

2. Theory of the Angular Dependency of Backward Radiated Ultrasonic Waves

Backward radiation is the leaky energy return-ing to a single transducer along the incident direction from the backward propagating leaky surface wave, which is converted from the for-ward surface wave generated in the incidence surface region of substrate. The profile of back-ward radiation will be affected by various factors such as beam directivity, frequency characteristics of transducer, dispersion and scattering of surface wave (Kwon et al., 2000). In principle, severe dispersion corresponds to a wide backward radia-tion profile, and the peak intensity is inversely proportional to the radiation width due to the band-pass filtering function. Angular profile of backward radiation amplitude, A_B, was expressed as given in Eq. (1) (Kwon et al., 2000).

$$A_B(\theta_i) = A \int_0^\infty T(f) C(f, d) D[\theta_i - \theta(f)]^2 df. \quad (1)$$

where f is frequency, A is a constant, $T(f)$ represents the frequency characteristics of transducer, θ_i denotes the incidence angle of beam center, $D(\theta)$ represents the directivity of transducer, $C(f, d)$ is the conversion function from forward to backward wave, d is the scatter size, and $\theta(f)$ is the angular dispersion function.

More detailed explanation for these parameters can be found in Kwon et al., (2000).

3. Procedures of Wear and Fatigue Tests

3.1 Wear test

The surface of many mechanical parts does not only degrade due to wear of materials, but may also suddenly progress toward catastrophic sur-face failure (Ludema, 1984), which is called the scuffing defined here as sudden departure from proper functioning of lubricated sliding pairs. However, a surface can be made sustain very severe loading condition if relatively low load is applied for a short period of time (Lee, and Ludema, 1990). This early stage of treatment is called the break-in, and it has been found that it involves formation of compressive residual stresses on and below the sliding surface.

For this reason, it is required to study the scuffing mechanism that should be related to processes occurring below the surface. Under the condition of good lubrication, the distribution of the residual stresses on and below the sliding surface might be a useful parameter for deter-mining the occurrence of scuffing and for study-ing the relationship between the break-in and scuff-life.

For wear tests, disks of AISI 1045 steel with thickness of 9 mm and diameter of 60 mm were used as flat surfaces. The disks were oil-quenched from 870 ℃ and tempered to have the material properties shown in Table 1. Then the disks were polished in random directions, producing 0.3 mm in Ra, which is the arithmetic average roughness. AISI 52100 cylindrical bearings with diameter of 6 mm and length of 6 mm were used as the counter part. Contact was achieved by pressing the cylinder against the flat surface under a normal load applied by a spring force, which reduced the variation of normal force during sliding. Scuffing tests and break-in procedure were performed at room temperature with loading conditions shown in Table 2. Two types of scuffing test were carried out in order to verify the influence of break-in on the scuffing-failure time.

Table 1 Mechanical properties of disk and cylinder for sliding test

Properties	Disk	Cylinder
Hardness, HRC	29	66
Modulus of Elasticity, GPa	205	205
Yield Stength, MPa	650	2034
Tensile Strength, MPa	869	2240
Density, g/cc	7.85	7.81

Table 2 Loading conditions for sliding test

		Break-in	Scuffing
Rotating speed		93 rpm	136 rpm
Normal Load	Initial	100 N	
	Increasing rate	50 N/10 min	730 N
	Final	200 N	
Lubricant		Mineral oil	

During the sliding test, the disks were cleaned carefully with acetone, and the residual stresses on the sliding surface and subsurface were measured using the X-ray diffraction method along the sliding direction.

3.2 Fatigue test

In order to prevent materials from corrosion damages or to evaluate the service-life, it is essential to evaluate the corrosion degradation and fatigue characteristics of the materials in service environments (Tanaka, 1980). Thus, in this paper, the corrosion degradation and fatigue characteristics of the specimens degraded by corrosion for a long period were evaluated. For fatigue tests in air, specimens of 12Cr alloy steel with $63 \times 60 \times 13$ mm^3 were used. Table 3 lists chemical and mechanical properties of the material. In particular, since the notch tip might be blunted by corrosion during the period of artificial degradation, smooth specimen was prepared

for artificial degradation (Cho et al., 2000). During the artificial degradation process, pitting corrosion was controlled by precise polishing of the surface of the specimen. Test conditions for artificial degradation in distilled water were as follows : 1) the temperature of distilled water was set at 25 ℃, 60 ℃ and 90 ℃, and 2) the degradation period was 9 months for evaluating the degradation effect on the fatigue characteristics of the material. Submerging the test coupons in distilled water of the corrosion cell, the temperature was controlled using a thermo-controller (Cho, Kim and Bae, 2000). The fatigue tester used for each coupon that has been degraded in distilled water for established period is a material testing system MTS, 10 tons) and the fatigue tests were conducted with the frequency(f) of 20 Hz and the load ratio(R) of 0.1. The fatigue crack length was measured using a traveling microscope (×50).

4. Result and discussion

4.1 Wear and fatigue tests

The distribution of residual stress in specimens before sliding tests was in the range of ± 20 MPa up to 20 μm below the sliding surface. The value of ± 20 MPa would be negligible, and is assumed to be due to the polishing process.

After the sliding test, residual stress had different distributions depending on whether they were broken-in or not. The scuffing failure time was also different from each other as shown in Fig. 1. Though the specimen without break-in failed at 1360 cycles, the broken-in specimen survived eight times longer. Figure 2 shows the results of residual stress measurement for each case of sliding test. This showed significant increase in the compressive residual stress below the surface, especially at 5 μm depth after 1360 cycles in the

Table 3 Chemical composition and mechanical properties of specimen for fatigue test

Element	C	Si	Mn	P	S	Ni	Cr	Mo	Al	Cu
Content (%)	0.16	0.34	0.46	0.02	0.003	0.2	11.9	0.09	0.006	0.06

Ultimate tenaile strength (MPa)	Yield strength (MPa)	Elongation (%)	Hardness (Rc)
1205	989.4	13	38

specimen that was broken-in. For much longer sliding (10800 cycles), the surfaces just started to fail, but survived almost eight times longer than those without break-in. The compressive residual stress just before the failure at the surface was increased up to 300 MPa. From the scuffing test, it can be concluded that the break-in procedure plays a very important role in forming and increasing the distribution of residual stress at surface and subsurface during scuffing test, since an increase in the compressive residual stress means more possibility to overcome failures due to further sliding. However, the specimens failed at the point where the compressive residual stresses near the surface no longer increase.

To confirm that advantageous break-in effect was due to compressive residual stress, the hardness on the wear track was measured.

As shown in Fig. 3, there were no remarkable differences between the broken-in specimen and

that without break-in. Hardness after the break-in procedure was about HV 330 and that of scuffing tested surface, which was not broken-in, was about HV 325. And at 8 μm depth, their trend is similar to that of surface.
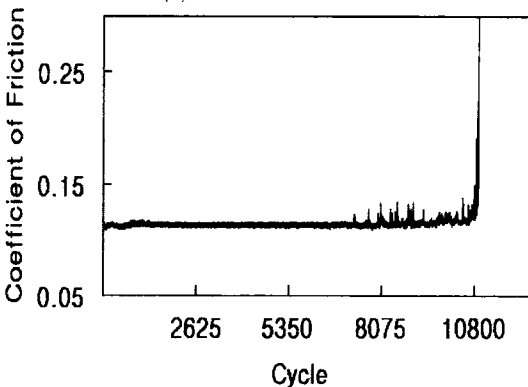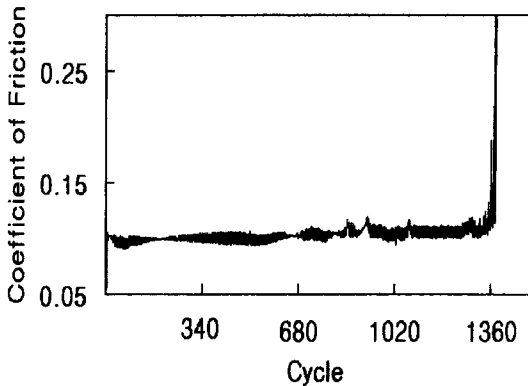

(a) After 1360 cycles without break-in

(b) After 1360 cycles with break-in

(c) After 10880 cycles without break-in

Fig. 2 Residual stress distribution after sliding test

(a) Without break-in

(b) With break-in

Fig. 1 Variation of friction coefficient up to scuffing
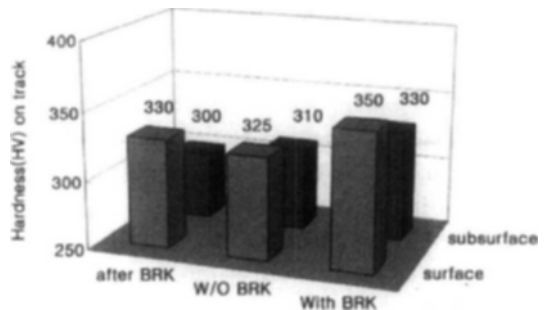
Fig. 3 Hardness on wear track after break-in and without break-in
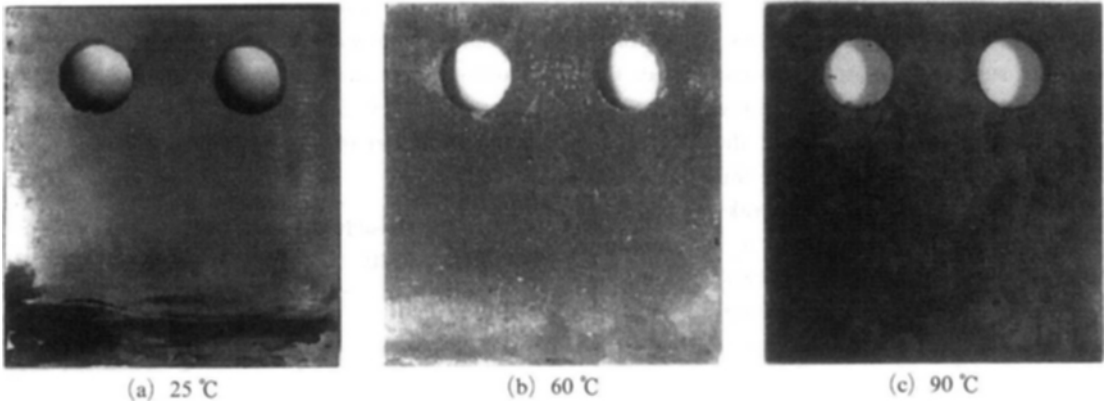
(a) 25 ℃   (b) 60 ℃   (c) 90 ℃

Fig. 4 Conditions of the outer surface on the coupons degraded for 9 months at 25 ℃, 60 ℃ and 90 ℃

So, It could be said that advantageous break-in effect in this experiment is not due to surface work hardening.

This means no more work hardening occurs at the surface and subsurface when the hardness of specimen reaches some limits as cycles pass by. So, we can say that all the three kinds of specimen were work hardened to almost the same degree, and only different in their residual stress distributions.

In the case of artificial degradation by corrosion, as an example, Fig. 4 shows the conditions of the outer surface of the coupons degraded for 9 months at 25 ℃, 60 ℃ and 90 ℃. The surface color of each coupon changed due to corrosion reaction and formation of corrosion products. These phenomena are due to the fact that the corrosion reaction increases according to the increase of the distilled water temperature.

Letting the material degrade in corrosive environment for a long period, the osmotic effect of surface corrosion by the continuous corrosion reaction can be predicted. Since these effects may, however, affect the fracture characteristics of the material, to obtain information on the degradation and failure of the material will be very important to secure the material reliability and safe design of industrial facilities.

Figure 5 shows the result that compares the in-air fatigue characteristics of the coupons which were artificially degraded for 3, 6 and 9 months in distilled water of 25 ℃, 60 ℃ and 90 ℃. Remarkable differences between them are not found. That
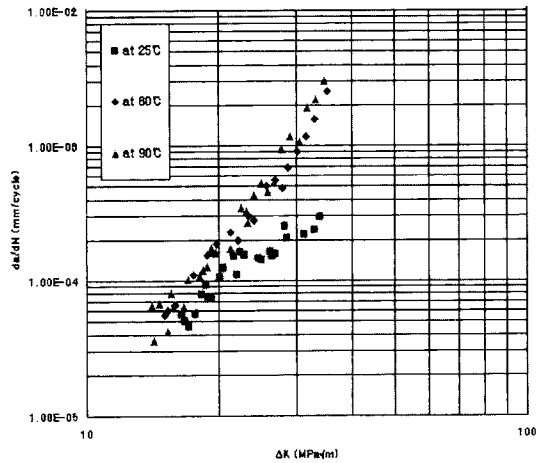

Fig. 5 Relationship between da/dN and K of 12Cr alloy steel degraded by corrosion in disfilled water of 25 ℃, 60 ℃ and 90 ℃ for 9 months

is, the degree of corrosion degradation during the test period in distilled water was not so large as to reduce the fatigue strength, and also to accelerate the fatigue crack growth rate of 12 Cr alloy steel.

4.2 Radiated backward ultrasonic measurement

The backscattering measurement setup is shown in Fig. 6. A broadband ultrasonic transducer (with the principal frequency of 4.7 MHz) was used to interrogate the specimen at different incidence angles. Incident angle was changed by the continuous movement of the probe at a constant angular speed, as shown in Fig. 6. To prevent the missing of high frequency compon-
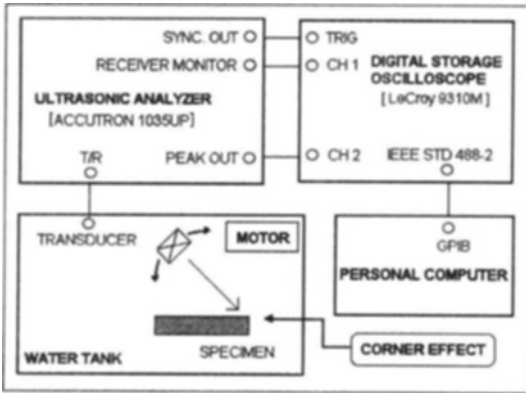
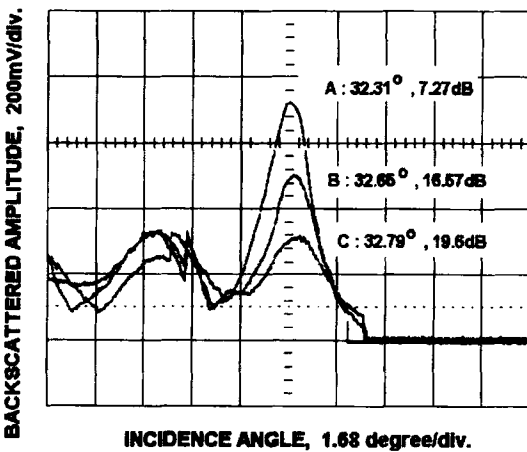**Fig. 6** Ultrasonic backscattering by corner effect and measuring system

Fig. 7 The difference in backward radiation profile in worn specimen

ents, the backward radiation was measured right at the corner of the specimen. This measurement scheme is named as the corner effect method.

Figure 7 shows the difference in the backward radiation profile in a worn specimen. Measurement was made on each specimen, after the break-in procedure, scuffing tested with break-in, and scuffing tested without break-in. The results show that the width of the backward radiation profiles was increased in the order listed above. The inversely proportional trend of the intensity of backward radiation to the width of the backward radiation coincides with the fact that the case having frequency dependency on the speed of surface wave has a wider range of angle, which

makes backward radiation possible, than that having no frequency dependency. It also coincides with the fact that the backward radiation energy at a specific angle decreases because only some part of frequency, which corresponds to the frequency dependency curve, can radiate. From Fig. 2, it can be noticed that specimen, after 1360 cycles, which was not broken-in have the steepest variation in subsurface, and the specimen, after 1360 cycles, which was broken-in has the least steep variation in the stress distributions. According to the perturbation theory, showing the change of frequency dependency curve, the more steeply properties change, the more the frequency dependency curve changes. So, it corresponds to the increase of the width of backward radiation and the decrease of intensity. However, applying the backward radiation peak in Fig. 7 to the Snell's law, the speed of surface wave that has maximum energy can be calculated. As a small angle means high speed, the calculated speed shows different values in wear tested specimens. It can be said that the speed of surface wave can indicate the amount of residual stresses existing near the surface. This means that by investigating the backward radiation profile, residual stress distribution can be evaluated and accordingly life of worn material can be evaluated.

Figure 8 shows the angular dependence of ultrasonic backscattering of 90 ℃ specimen. The left peak at 0 ° represents the normal incidence position. Smooth increase of backscattering near 17 ° is due to the creeping wave, that is a totally refracted longitudinal wave in substrate and backward scattered by corner effect. Increase shown at 34 ° is due to the backward radiation by the generation, scattering and leakage of Rayleigh waves. This profile shows sharp changes of peaks and an asymmetrical pattern, which are typical characteristics of backward radiation (Kwon et al., 2000). The asymmetry is due to the scattering of total refracted transverse waves so that the left side of radiation profile is wider and less smooth than the other side. Because the purpose in our experiment is to get the information of dispersion relation from the radiation profile, we took the right half width that was not affected by the
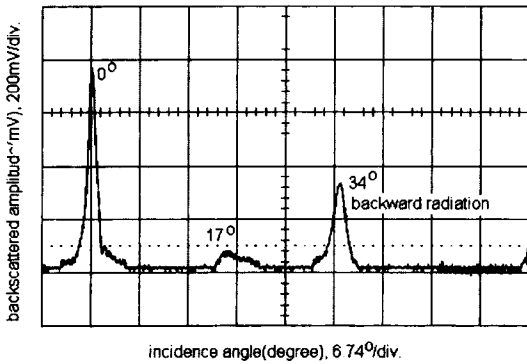
Fig. 8 Angular dependence of ultrasonic backscattering by corner effect involving the backward radiation of 90 ℃ specimen

transverse scattering.

Relationship between da/dN and $\triangle K$ in distilled water showed that crack growth characteristics were compared for different temperatures in Fig. 5. The exponent m and constant C in the Paris' law that can predict the crack size increment due to fatigue are presented in Table 4 with the parameters of backward radiation profile such as A_B (the peak intensity), v_R (Rayleigh wave velocity) and $\triangle\theta$ (the right-hand width). Here, it is worthwhile to note that A_B is defined as the absolute value of the intensity normalized by the reflected intensity at normal incidence. Thus, the smaller the value is, the greater the peak intensity is.

Normalized backward radiation profiles for 25 ℃, 60 ℃ and 90 ℃ specimens were peak-aligned and compared as shown in Fig. 9. The peak intensity increased with the corrosion temperature. Considering the asymmetry of the profile, the increase of scattering by corrosion is one of the possible reasons that A_B increased with temperature. However, it was asserted that the principal reason of this increase would be the decrease in angular distribution of the frequency spectrum energy. In other words, with the increase in corrosion temperature the frequency spectrum showed narrower distribution so that the peak intensity went higher due to the preservation of the total energy.

As shown in Fig. 9, the right-hand width of the profile $(\triangle\theta)$ linearly decreased as the corrosion

Table 4 Experimental estimation of C, m in Paris' law, A_B, v_R and $\triangle\theta$

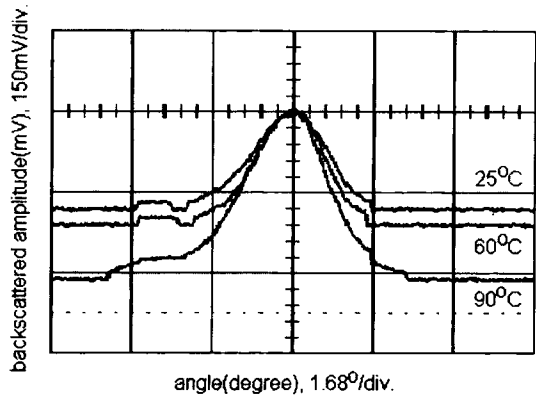| Specimen Temperature (℃)	v_R (m/s)	C ($\times 10^{-10}$)	m	A_B	$\triangle\theta$
25	2823.2	936	2.23	12.34	1.07
60	2796.6	8.00	3.55	11.04	0.89
90	2628.8	3.00	4.49	7.42	0.73

Fig. 9 Comparison of normalized backward radiation profile for 25 ℃, 60 ℃ and 90 ℃ specimens

temperature increased. However, the left-hand width, being affected by the surface roughness and micro cracks, did not show such a linearity. On the contrary, it showed the similar trend to the constants C in Paris' law. (As shown in Table 4, the constants C of 60 ℃ and 90 ℃ specimens are in the same order. However, that of 25 ℃ specimen is very large compared to them. The same trend can be clearly seen in the left-hand width as shown in Fig. 9.) Table 4 shows the right-hand width $(\triangle\theta)$ at 5dB. The decrease of this value implies less variation of velocity dispersion curve. The subsurface gradients by corrosion aging will typically behave as an exponential function but in order to discuss the relation between the gradient and dispersion, we simply assume an effective degraded layer. The surface wave velocities of high temperature specimens undergoing severe degradation showed less value than those of low temperatures. The result could be explained by recalling that the effective degraded layer with
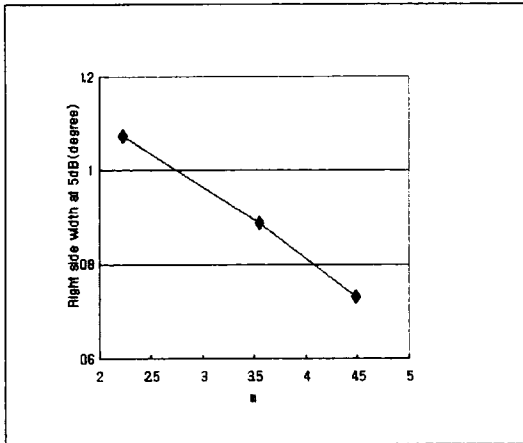
Fig. 10 m in Paris law versus the variation of right-hand half width at 5dB of backward radiation profile

less acoustic impedance was loaded (Lee, Oh, Nam, and Lee, 1999). In such a circumstance the dispersion curve and its slope decrease with the value of frequency multiplied by thickness of the effective layer; starting from the velocity of unperturbed specimen (with the degraded layer thickness of zero) to the effective layer velocity (Szabo, 1975). It is easily recognized that higher corrosion temperature yields greater layer thickness, which corresponds to the less slope in dispersion curve and the less profile width (Kwon and Kim, 1987).

Figure 10 shows the relation between m in the Paris' law and the width of backward radiation profile. The value m was inversely and linearly proportional to the width. It is certain that the change of degraded layer thickness affects the crack growth rate in the fatigue test. The linearity shown in Fig. 10 supports the conclusion that the measurement technique of degraded thickness or subsurface gradients using backward radiation profiles can be used for nondestructive evaluation of corrosion strength.

5. Conclusion

For nondestructively evaluating the degradation degree of materials, the frequency dependency of Rayleigh surface wave was investigated.

The subjects of investigation are wear and corrosion. In the case of wear, AISI 1045 steel was tested to measure the residual stress distribution between the broken-in specimen and that without break-in. In the case of corrosion, 12Cr alloy steel coupons degraded in distilled water of different temperatures for 9 months were tested to evaluate the degradation degree by corrosion and the fatigue characteristics.

The obtained conclusions are summarized as follows :

(1) The width of backward radiation profile decreases with the increase of the aging temperature. This means that the slope of dispersion curve at high temperature is less than that at low temperature, which seems to result from the increase of the effective degrading layer thickness.

(2) Different residual stress distribution was caused by the break-in process. Consequently, the residual stress increased below the surface, the region that could be mostly influenced by severe conditions of sliding, and the broken-in specimen could survive longer than raw specimen did. The peak intensity of the backward radiation profile decreases and the right-hand half width of the profile increases with the increase in the variation of residual stress distribution for the scuffing specimen.

(3) The radiation width also shows an inverse proportionality to the exponent, m, in the Paris' law which is an indicator of the crack growth characteristics due to fatigue.

(4) The result observed in this study demonstrates high potential of the backward radiated ultrasound as a tool for nondestructive evaluation of not only the corrosion-fatigue characteristics of the aged materials but also subsurface gradients of the surface residual stress by scuffing.

Acknowledgment

References

Bertoni, H. L. and Tamir, T., 1973, "Unified Theory of Rayleigh angle Phenomena for Acoustic Beam at Liquid-Solid Interfaces," *Applied Physics*, Vol. 2, pp. 157~172.

Cho, S. Y., Kim, C. H. and Bae, D. H., 2000, "A Study on the Corrosion Fatigue Characteristics of 12Cr Alloy Steel," *Key Engineering Materials*, Vol. 183, pp. 993~998.

Kim, H. C., Lee, J. K., Kim, S. Y. and Kwon, S. D., 1999, "Influence of Microstructure on the Ultrasonic Backscattered energy from a liquid/solid interface at the Rayleigh angle," *Japanese Journal of Applied Physics*, Vol. 38, No. 1, pp. 260~267.

Kwon, S. D. and Kim, H. C., 1987, "Dispersion of Acoustic Surface Waves by Velocity Gradients," *Journal of Applied Physics*, Vol. 62, pp. 2660~2664.

Kwon, S. D., Choi, M. S., and Lee, S. H., 2000, "The Applications of Ultrasonic Backward Radiation from a Layered Substrate Submerged in Liquid," *NDT & E International*, Vol. 33, No. 5, pp. 275~281.

Lee, K. C., Oh, J. H., Nam, K. W. and Lee, J. S., 1999, "Nondestructive Evaluation by Joint Time-Frequency Analysis of Degraded SUS 316 Steel," *Journal of Kor. Soc. for Nondes. Testing*, Vol. 19, No. 4, pp. 270~276.

Lee, Y. Z. and Ludema, K. C., 1990, "The Shared Load Wear Model in Lubricated Sliding: Scuffing Criteria and Wear Coefficient," *Wear*, Vol. 138, pp. 13~19.

Ludema, K. C., 1984, "A Review of Scuffing and Running-in of Lubricated Surface with Asperities and Oxides in Perspective," *Wear*, Vol. 100, pp. 315-331.

Szabo, T. L. 1975, "Obtaining Subsurface Profiles from Surface Acoustic Wave Velocity Dispersion," *Journal of Applied Physics*, Vol. 46, No. 4, pp. 1448~1454.

Tanaka, T. O. 1980, "Practice and Policy for Fracture under Wet H2S Environment," *Fracture of Metals*, Syohwa Print, pp. 155-166.

Viktorov, I. A., 1967, Rayleigh and Lamb Waves, Plenum Press, New York.